Draft version November 8, 2015
Preprint typeset using LaTeX style emulateapj v. 12/01/06

MASS ESTIMATES OF AN ULTRA-FAINT GALAXY AND AN OUTER HALO GLOBULAR CLUSTER: BOÖTES II AND ERIDANUS

Marla Geha[1], Joshua D. Simon[2], Ricardo Muñoz[3], Evan Kirby[4], and other people.

Draft version November 8, 2015

ABSTRACT

We present dynamical massess and improved photometric properties for the Milky Way ultra-faint galaxy Boötes II (Boo II) and the halo globular cluster Eridanus (Eri) based on Keck/DEIMOS spectroscopy and deep CFHT imaging. These two objects have similar luminosities, but very different structure, kinematics and chemistries. From 20 member stars, we estimate the velocity dispersion of Boo II to be $\sigma = 2.0^{+1.3}_{-1.1}$ km s^{-1}. Based on 34 member stars in Eridanus, we can only place an upper limit on the velocity dispersion of $\sigma < 0.7$ km s^{-1}. Combining the photometric and kinematic observations, we infer the mass of Boo II inside the half-light radius is $M_{1/2} = 5.5^{+2.8}_{-2.8} \times 10^5\ M_\odot$, corresponding to a $M/L_V = 445 \pm 300$. The mass of Eridanus is $M_{1/2} < 3.8 \times 10^3\ M_\odot$, corresponding to a $M/L_V < 1$. The mass-to-light ratio of Eri is consistent with that of a normal old stellar populations, in contrast to Boo II which is difficult to interpret without a significant dark matter component. The mean metallicity of Boo II is $<[Fe/H]> = -1.9 \pm 0.2$, with an internal metallicity dispersion of 0.5 dex. The mean metallicity of Eridanus is $<[Fe/H]> = -1.0 \pm 0.1$, with no measurable metallicity spread. The different kinematics and chemistries of Boo II and Eri are a clean demonstration that, in most cases, globular clusters and ultra-faint galaxies are two well separated classes of objects.

Subject headings: galaxies: dwarf — galaxies: kinematics and dynamics — galaxies: individual (Boo II) Galaxy: globular clusters: individual (Eridanus)

1. INTRODUCTION

The discovery of the ultra-faint satellites around the Milky Way (Simon & Geha 2007), has blurred the distinction between dwarf galaxies and globular star clusters (Willman & Strader 2012). This delineation was most obvious in the relationship between total luminosity and physical size: at a given total luminosity, globular clusters tend to be more concentrated than dwarf galaxies, with an order of magnitude smaller characteristic radii (Belokurov et al. 2006). Dwarf galaxies were further differentiated from globular clusters as having significant dark matter content and a substantial internal spread in metallicity, possibly suggesting multiple epochs of star formation. This is in contrast to globular clusters which shown little evidence for dark matter (**?**).

In the few cases where the age or metallicity spread is substantial (Omega Cen;), these objects are assumed to have a different origin than the bulk of the cluster population, such as remnants of tidally stripped dwarf galaxies

While the above definitions still hold, the ultra-faint galaxies have blurred the distinction between globular clusters and dwarf galaxies. The ultra-faint galaxies have absolute magnitudes fainter than $M_V > -8$ and have only been recently discovered as resolved over-densities of stars. The faintest of these discoveries have the smallest known sizes for any .

Because the faintest galaxies can so far only be found near the Milky Way (< 50 kpc), these objects are also the most susceptible to the tidal forces of the Milky Way. It has thus been suggested that the ultra-faint galaxies are instead globular clusters which have been caught in

[1] Astronomy Department, Yale University, New Haven, CT 06520. marla.geha@yale.edu

In this paper, we present Keck/DEIMOS spectroscopic and CFHT/MegaCam photometric measurements for two objects with similar luminosities: Boötes II and Eridanus. We show that the kinematic properties and metalicity distribution of these two objects are very different, consistent with the interpretation that Boötes II is an ultra-faint galaxy, while Eridanus is a globular cluster. The paper is organized as follows: in § 2 we discuss target selection, data reduction and member selection for our Keck/DEIMOS spectroscopy.

2. DATA

We present data for the Milky Way satellites Boötes II (Boo II) and Eridanus (Eri). Both objects have limited photometric and spectroscopic data in the literature. Boo II was discovered by Walsh et al. (2007) in SDSS imaging, and classified as an ultra-faint galaxy at ~~roughly~~ 40 kpc. Eridanus was found in ESO Schmidt plates and subsequently classified as a globular cluster at ~~roughly~~ 90 kpc (Cesarsky et al. 1977). Both classifications are based on the combined photometric ~~radius~~ and luminosity. paper has only.

2.1. *Photometry: Structural Parameters*

We obtained deep Canada-France-Hawaii Telescope (CFHT) MegaCam g- and r-band imaging of Boo II and Eri in April 2010 and October 2009, respectively. These data were taken as part of a larger photometric survey of Milky Way satellites (PI: Coté) which will be described in a future paper (R. Muñoz et al. 2016, in prep.). Each object was observed for a total of one hour, split roughly equal between the two filters. Image reduction is the same as that described in Muñoz et al. (2010), and includes standard calibrations and photometry using DAOPHOT/Allframe (Stetson 1994). In the case of Boo II, the photometry was calibrated against

overlapping bright stars in the SDSS Data Release 7 (**?**, DR7). Eri is not in the SDSS DR7 footprint and was instead calibrated against BVI standard field photometry in the cluster's center from P. Stetson's online database[†], and the photometric transformation of **?**. Final color-magnitude diagrams are shown for each object in the left panels of Figures 1 and 2.

Both Boo II and Eri are sufficiently low luminosity that even our deep CFHT photometry detects only a few hundred individual stars belonging to each object. We therefore determine the total luminosity, half-light radii and ellipiticity of Boo II and Eri using the maximum likelihood methods described in Muñoz et al. (2010). This method is a significant improvement over traditional surface brightness fitting algorithms in the case of low numbers of resolved stars (Martin et al. 2008; **?**). The method relies solely on the total number of stars belonging to the satellite and not on their individual magnitudes (Muñoz et al. 2010). To estimate an absolute magnitude, we modelled an object's population with the best-fitting theoretical luminosity function, in this case a 12 Gyr population with [Fe/H]$= -1.5$ (Girardi et al. 2002). We then integrated the theoretical luminosity function assuming a Kroupa IMF to obtain the total flux down to a given magnitude limit.

For Boo II, we determine a total luminosity of $M_V = -2.9 \pm 0.7$ and half-light radius of $3.0 \pm 0.5'$ (37 ± 6 pc). These values are within the 1-sigma errors of the same values computed by **?** and **?**. We redetermine the distance of Boo II using our deeper photometry and method described above, confirming the distance determined in **?** of 42 ± 8, which is closer than in the Walsh et al. (2007) discovery paper.

For the globular cluster Eri, we determine a total luminosity of $M_V = -4.9 \pm 0.3$ and half-light radius of $r_{\rm eff} = 0.64' \pm 0.04$ (16.7 ± 1.1 pc). Our half-light radius of Eri is a factor of 2 larger than the previously determined size based on significantly shallower Palomar Sky Survey plates (Ortolani & Gratton 1986; Harris 1996). The photometric properties of both objects are listed in Table 1.

2.2. *Target Selection*

Target stars for Keck/DEIMOS spectroscopy were selected based on g- and r-band photometry. In the case of Eri, we used the CFHT photometry described above. For Boo II, target selection was done using the SDSS DR7, as the CFHT imaging was not available at the time. Because targets are only selected for spectroscopy down to $r = 22$ mag, the SDSS photometry was sufficient for this purpose. Using the Girardi et al. (2002) isochrones, we chose targets whose color and apparent magnitudes minimize the distance from the best fitting isochrone at the distance of each object. The highest priority targets were those located within 0.1 mag of the RGB or AGB tracks, or within 0.2 mag of the MS and horizontal branch, with additional preference being given to brighter stars (see SG07 for details). Stars farther from any of the fiducial sequences were classified as lower priority targets. Slitmasks were created using the DEIMOS `dsimulator` package.

[†] http://cadcwww.dao.nrc.ca/community/STETSON/standards/

2.3. *Spectroscopy and Data Reduction*

Spectroscopy for individual stars in Boo II and Eri was obtained with the Keck II 10-m telescope and the DEIMOS spectrograph (Faber et al. 2003). Five multi-slit masks were observed for Boo II on the nights of 2009 Febraury 19 and 28 and 2010 February 14, and two multi-slits masks were observed for Eri on 2010 February 13-14. Field positions and exposure times are listed in Table 2. The masks were observed through the 1200 line mm^{-1} grating covering a wavelength region $6400 - 9100$ Å. The spatial scale is $0.12''$ per pixel, the spectral dispersion of this setup is 0.33 Å, and the resulting spectral resolution is 1.37 Å (FWHM). Slitlets were $0.7''$ wide. The minimum slit length was $5''$ to allow adequate sky subtraction; the minimum spatial separation between slit ends was $0.4''$ (three pixels). Spectra were reduced using a modified version of the `spec2d` software pipeline (version 1.1.4) developed by the DEEP2 team at the University of California-Berkeley for that survey (Newman et al. 2012). A detailed description of the two-dimensional reductions can be found in SG07. The final one-dimensional spectra are rebinned into logarithmic wavelength bins with 15 km s^{-1} per pixel.

Radial velocities were measured by cross-correlating the observed science spectra with a set of high signal-to-noise stellar templates. The method is the same as that described in SG07 and briefly repeated here. Stellar templates were observed with Keck/DEIMOS using the same setup as described in § 2.3 and covering a wide range of stellar types (F8 to M8 giants, subgiants and dwarf stars) and metallicities ([Fe/H] $= -2.12$ to $+0.11$ dex). We calculate and apply a telluric correction to each science spectrum by cross correlating a hot stellar template with the night sky absorption lines following the method in Sohn et al. (2006). The telluric correction accounts for the velocity error due to mis-centering the star within the $0.7''$ slit caused by small mask rotations or astrometric errors. We apply both a telluric and heliocentric correction to all velocities presented in this paper.

The random component of the velocity error is calculated using a Monte Carlo bootstrap method. Noise is added to each pixel in the one-dimensional science spectrum, we then recalculate the velocity and telluric correction for 1000 noise realizations. The random error is defined as the square root of the variance in the recovered mean velocity in the Monte Carlo simulations. The systematic contribution to the velocity error was determined by SG07 to be 2.2 km s^{-1} based on repeated independent measurements of individual stars, and has been subsequently confirmed with a much larger sample of repeated measurements. We add the random and systematic errors in quadrature to arrive at the final velocity error for each science measurement. The fitted velocities were visually inspected to ensure reliability.

2.4. *Repeat Velocity Measurements*

We obtained repeated velocity measurements for a handful of stars in each system as a check on our systematic error and to possibily detect binary stars which might affect the velocity dispersion of these systems. In Eri, we obtained repeat measurements only for two non-members stars separated by one day. The measured velocities are within the one-sigma errors of each other.

In Boo II, we obtain repeat measurements for 8 member stars. Repeat observations are separated by as much as one year. The most significant velocity variations was observed in the star SDSS J135807.04+125122.8 which varied by 20 km s^{-1} in three measurements (3-sigma deviations). The color, magnitude and amplitude of the velocity variation of this star is consistent with being an RR Lyrae star (Figure 1). We identify this star as a member of Boo II, but do not use it in our velocity analysis due to its uncertain systemic velocity. Of the remaining seven member stars with repeat measurements, one star shows a velocity difference within 2-sigma and the velocities of six stars are constant within one-sigma errors. In these cases, we use the weighted averages of these multiple measurements.

? identified the star J135751.2+125137.0 as a spectroscopic binary system. While we did not get repeat velocities for this object with DEIMOS, our measurement of this star is several sigma from the Boo II systematic velocity. Removing this single star from the membership sample dramatically reduces the measured velocity dispersion of the overall system: from 4.0 ± 1.0 km s^{-1}to the 2.0 ± 1.2 km s^{-1}estimated in § 3.1. Removal of no other single star influences the velocity dispersion by one sigma. Therefore, we agree with the assessment of **?** and remove this object from our kinematic analysis below.

2.5. *Membership Selection Criteria*

Membership selection for both Boo II and Eri is based on combined photometric and kinematic criteria. We first photometrically select stars based on the CFHT photometry to be within 0.2 mag of the best fitting isochrone for each object. For stars passing this photometric cut, we select members based on their radial velocity. The velocity histograms in the right panel of Figures 1 and 2 show clear velocity peaks well in excess of that predicted by models of the Besançon Milky Way at these velocities (Robin et al. 2003). We use this peak as the initial guess of the system's systemic velocity and apply a generous velocity cut of 15 km s^{-1} around this peak. While this velocity window is three or more times the velocity dispersion, no stars passing both the CMD and kinematic cut are further than two sigma from the inferred velocity and we therefore do not further refine our selection criteria. We note that the improved CFHT photometry substantially reduces the uncertainty in membership selection as compared to previous spectroscopic studies of comparable systems which used SDSS photometry (**?**Geha et al. 2009; Simon et al. 2011).

The final samples for Boo II and Eri contain 22 and 32 member stars, respectively. The color-magnitude and velocity distribution of kinematically-selected members are shown in Figures 1 and 2. For stars identified as members of Boo II or Eri, the individual velocities and associated errors are listed in Table 3.

3. RESULTS

We have observed Eri and Boo II both photometrically and spectroscopically through identical observational setups, reduction and analysis tools. The final member samples have comparable numbers of stars. In addition to presenting the first velocity dispersion of the globular cluster Eri and a significantly improved measurement for the velocity dispersion of Boo II, a goal of this paper is to highlight the clear observational differences between globular clusters and ultra-faint galaxies in the region where the structural properties of these objects overlap.

TABLE 1
Observed and Derived Quantities for Boo II and Eri

Row	Quantity	Units	Boo II	Eri
(1)	RA	h:m:s	13:58:03.4±1.9	04:24:44.5±0.1
(2)	DEC	° : ′ : ″	+12:51:19±21″	−21:11:15±1.5″
(3)	E(B-V)	mag	0.031	0.021
(4)	Dist	kpc	42 ± 8	90.1
(5)	$M_{V,0}$	mag	-2.9 ± 0.7	-4.9 ± 0.3
(6)	$L_{V,0}$	$L_\odot$	$1614^{+406?}_{-235?}$	9817^{+1187}_{-900}
(7)	ϵ		0.24 ± 0.12	0.09 ± 0.04
(8)	$\mu_{V,0}$	mag ″$^{-2}$	$27.9^{+1.0}_{-0.7}$	23.6
(9)	$r_{\rm eff}$	′	3.0 ± 0.45	0.64 ± 0.04
(10)	$r_{\rm eff}$	pc	$37? \pm 5.5$	$16.7? \pm 1.1$
(11)	v	km s^{-1}	-128.3 ± 1.3	-18.3 ± 0.5
(12)	$v_{\rm GSR}$	km s^{-1}	114 ± 2	185
(13)	σ	km s^{-1}	4.3 ± 1.2	< 0.7
(14)	Mass	$M_\odot$	$4.3^{+4.7}_{-2.5} \times 10^5$	
(15)	M/L	$M_\odot / L_\odot$	1340^{+4340}_{-990}	
(16)	[Fe/H]	dex	-1.87 ± 0.17	-1.11 ± 0.04
(16)	$\sigma_{[Fe/H]}$	dex	0.5 ± 0.1	< 0.1

Note. — Columns (1)-(2) and (4)-(10) dervied from CFHT imaging as described in Munoz et al. Column (3) from Schlegel et al. (1998). Columns (11)-(13) are derived in xx.

3.1. *Velocities and Velocity Dispersions*

Given the member stars identified in § 2.5, we measure the mean velocity and velocity dispersion of Boo II and Eri using the MCMC algorithm described in § **??**.

The mean heliocentric velocity of Boo II is determined to be $v = -129.0 \pm 1.1$ km s^{-1} with a velocity dispersion of $\sigma = 4.4 \pm 1.0$ km s^{-1}. These values are in consistent with, but more accurate than, Koch et al. (2008) who measured 5 velocities stars in this object.

The mean heliocentric velocity of the globular cluster Eri is $v = -19.1 \pm 0.5$ km s^{-1}. This is consistent with published kinematic measurements of Eri of $v = -21 \pm 4$ km s^{-1} based on three stars (Zaritsky et al. 1989). From our full member sample of 32 stars, we find a mean velocity dispersion of 1.5 ± 0.8 km s^{-1}. While the internal dispersion of this cluster has not been previously measured, our value agrees with the velocity dispersion predicted by Gnedin & Zhao (2002) of 1.3 km s^{-1}, based its photometric properties: a single-mass isotropic King models with a constant mass-to-light ratio $M/L_V = 3$. We discuss the dynamical mass and mass-to-light ratio of Eri further below.

3.2. *Mass and Mass-to-Light Ratio*

We determine the dynamical mass of Boo II and Eri enclosed within the half-light radius applying the formula from Wolf et al. (2010): $M_{1/2}(\mathrm{r}_{1/2}) \simeq 4\mathrm{G}^{-1}\langle\sigma^2_{\rm los}\rangle \mathrm{r}_{1/2}$, where $M_{1/2}$ is the mass contained within the 3D projected half-light radius, $\sigma_{\rm los}$ is the line-of-sight velocity dispersion. This mass estimator is based on the Jeans Equation and is less sensitive to uncertainties in the velocity anisotropy than other simple mass estimates. We calculated an enclosed mass for Boo II of $M_{1/2} = 6.5^{+x}_{-x} \times 10^5\, M_\odot$ and Eri of $M_{1/2} = 1.3^{+2.7}_{-1.3} \times 10^3\, M_\odot$.

Using the luminosity determined in § 2.1, we determine the dynamical mass-to-light ratio for each object.

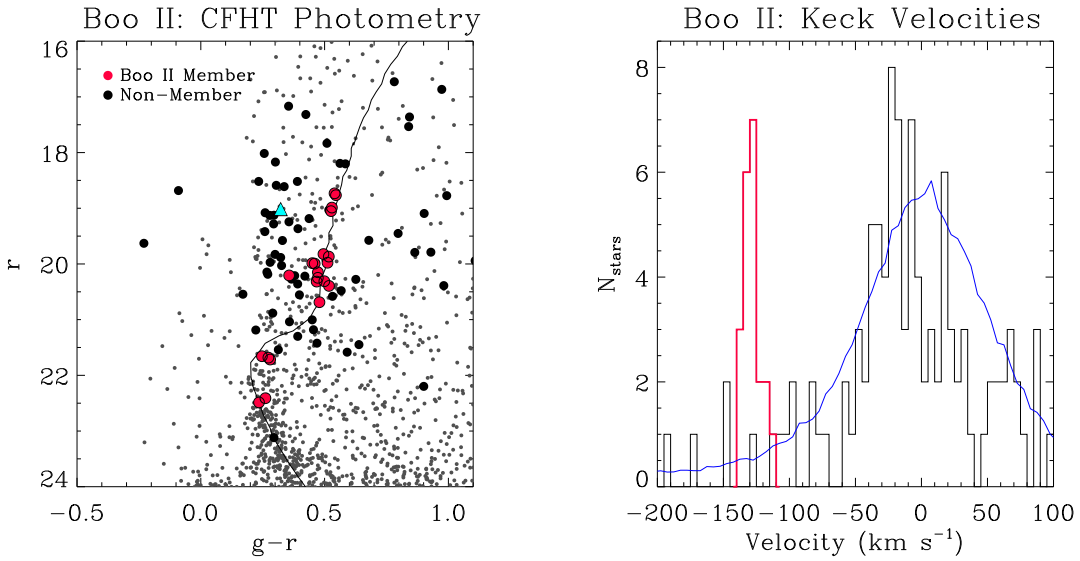

FIG. 1.— *Left:* Color-magnitude diagram of all stars (small grey points) within 10′ of the center of Boo II from CFHT photometry. The larger symbols indicate stars with measured Keck/DEIMOS velocities: red symbols fulfill our requirements for membership in Boo II, large black symbols are foreground Milky Way stars. A fiducial isochrone (Girardi et al. 2002) is shown shifted to the distance of Boo II. *Right:* Velocity histogram of spectroscopic targets for Boo II. Selected member stars are shown in red.

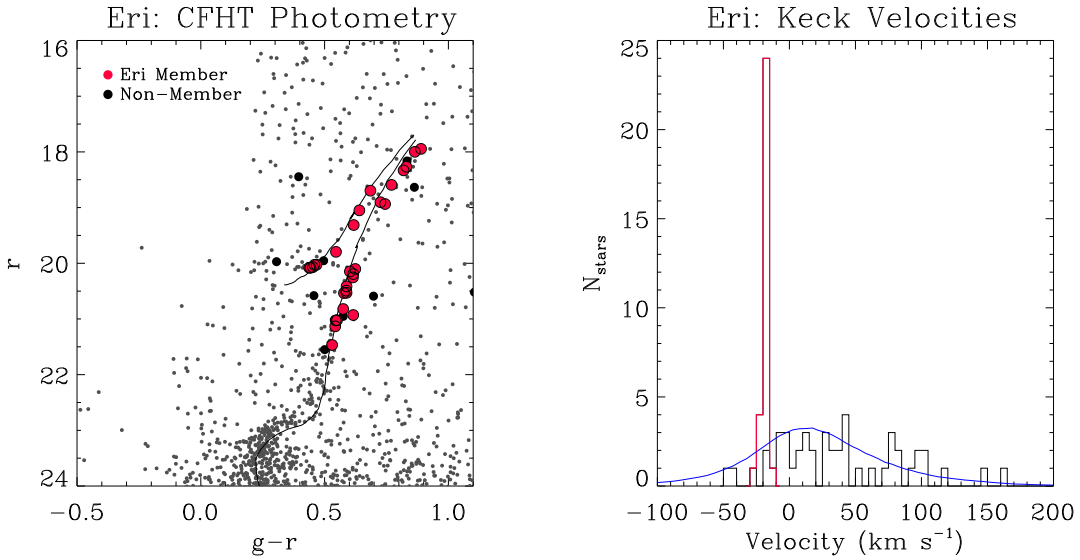

FIG. 2.— Same as Figure 1 for the globular cluster Eri.

Starting with Eri, we calculate a mass-to-light ratio = $\Upsilon_V = 2.4^{+5.0}_{-2.4}\, M_\odot / L_\odot$. Based on a single age old stellar population consistent with the metallicity of Eri ([Fe/H] = x), we expect a mass-to-light ratio between 2-3. Inverting the Wolf et al. formula, we would predict a velocity dispersion between x and y based on the stellar mass alone. Our observations are fully consistent with the conclusion that Eri is a globular cluster whose stellar mass is consistent with its dynamical mass.

For Boo II, we calculate $\Upsilon_V = 2.4^{+5.0}_{-2.4}\, M_\odot / L_\odot$. This is well in excess of the mass-to-light ratio expected for any stellar population. Again inverting the Wolf et al. formula using a reasonable stellar mass-to-light ratio, we predict a velocity dispersion of xx, several sigma below our measurements. Thus, while the dynamical mass of Eri is consistent with its stellar mass, we infer a significant amount of dark matter in Boo II.

The above statement assumes both systems are in dynamical equilibrium. [look at any possible tidal effects].

3.3. *Metallcity Distributions*

We estimate the spectroscopic metallicity of individual stars in our member samples via the spectral synthesis modeling method desribed in Kirby et al. (2008). This method compares the observed spectrum to a grid of synthetic spectra covering a range of effective temperature, surface gravity and composition. Photometry is used to estimate effective temperature and surface gravity for each star. The best matching composition is found by minimizing residuals between the observed spectrum and a smoothed synthetic spectrum matched to the DEIMOS spectral resolution. Although it is possible to determine

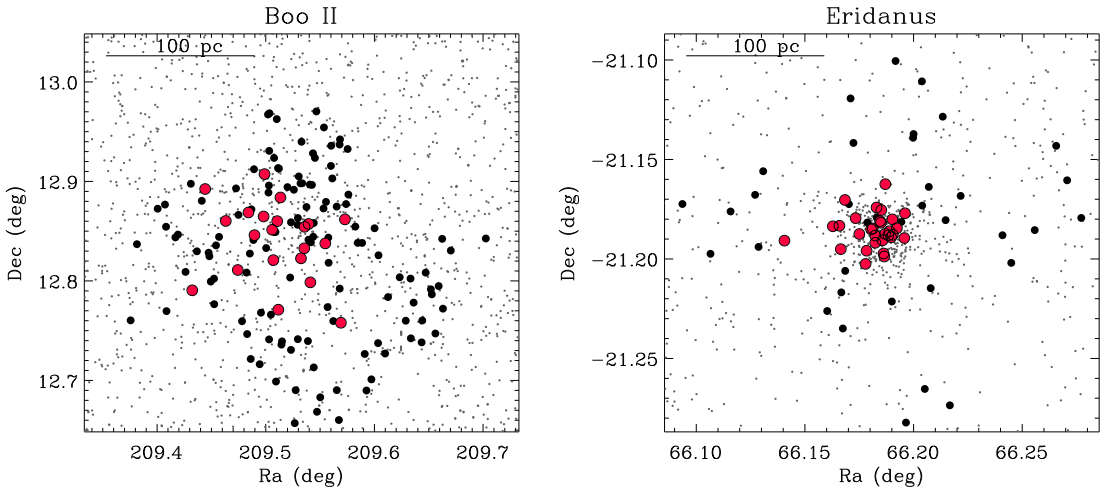

FIG. 3.— *Left:* Spatial distribution of stars near Boo II. Small points are all stars in this region, larger symbols indicate stars with Keck/DEIMOS spectroscopy, with red symbols showing confirmed members of Boo II. The solid ellipse is the half-light radius of this object. *Right:* Same figure, but for the globular cluster Eri.

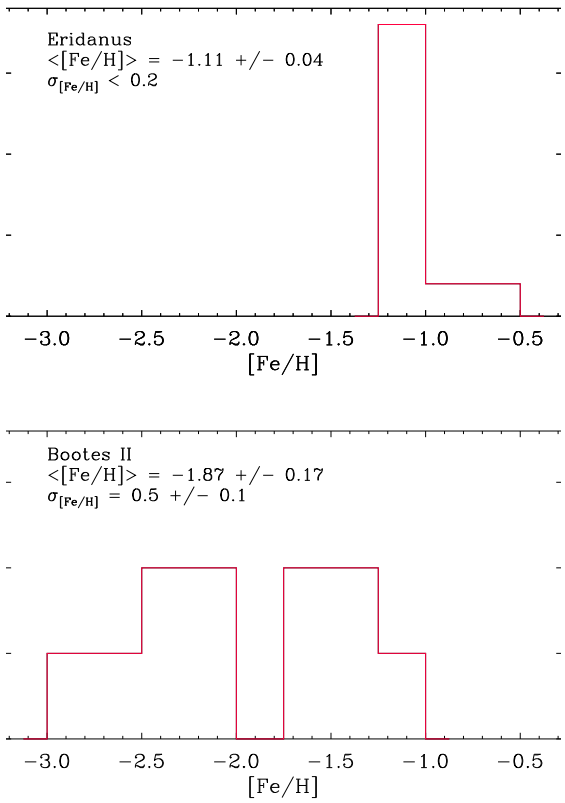

FIG. 4.— Metalicity distribution of member stars in Eri (*top*) and Boo II (*bottom*). The globular cluster Eri is consistent with a single metallicity stellar population with [Fe/H] $= -1.11 \pm 0.04$, while the ultra-faint galaxy Boo II has a significant internal metallicity dispersion ($\sigma = 0.5 \pm 0.1$ dex) with an average of [Fe/H]$=-1.87 \pm 0.17$.

both [Fe/H] and [α/Fe] via this method, we focus on only [Fe/H] in this paper. We mask α element lines and fix the model atmospheres at [α/Fe] $= +0.2$.

The metallicity distribution for Boo II and Eri are shown in Figure 4. For Boo II, we determine an average metallicity of [Fe/H] $= -1.87 \pm 0.17$ with and internal dispersion of 0.5 ± 0.1 dex. For Eri, we determine an average metallicity of [Fe/H] $= -1.11 \pm 0.04$ with no internal dispersion. This is consistent with the interpretation that Eri is a globular cluster with a single stellar population, while Boo II is a galaxy with multiple metallicity populations.

Deep photometry of this object suggests a metallicity of [Fe/H] $= -1.42$ (Stetson et al. 1999), which agrees with the spectroscopic metallicity determined for two stars of [Fe/H]$= -1.41 \pm 0.11$ (Armandroff & Da Costa 1991).

4. DISCUSSION AND CONCLUSIONS

The radial velocity of Boo II is significantly different than that of another ultra-faint galaxy Boötes I which lies less than 2° (away, but at a velocity of 96± km s^{-1}(Muñoz et al. 2006). Thus, as first suggested by Koch et al., Boötes I and Boo II are not physically associated with each other.

REFERENCES

Armandroff, T. E. & Da Costa, G. S. 1991, AJ, 101, 1329
Belokurov, V., Zucker, D. B., Evans, N. W., Gilmore, G., Vidrih, S., Bramich, D. M., Newberg, H. J., Wyse, R. F. G., Irwin, M. J., Fellhauer, M., Hewett, P. C., Walton, N. A., Wilkinson, M. I., Cole, N., Yanny, B., Rockosi, C. M., Beers, T. C., Bell, E. F., Brinkmann, J., Ivezić, Ž., & Lupton, R. 2006, ApJ, 642, L137
Blanton, M. R. 2006, ApJ, 648, 268
Cesarsky, D. A., Lequeux, J., Laustsen, S., Schuster, H.-E., & West, R. M. 1977, A&A, 61, L31

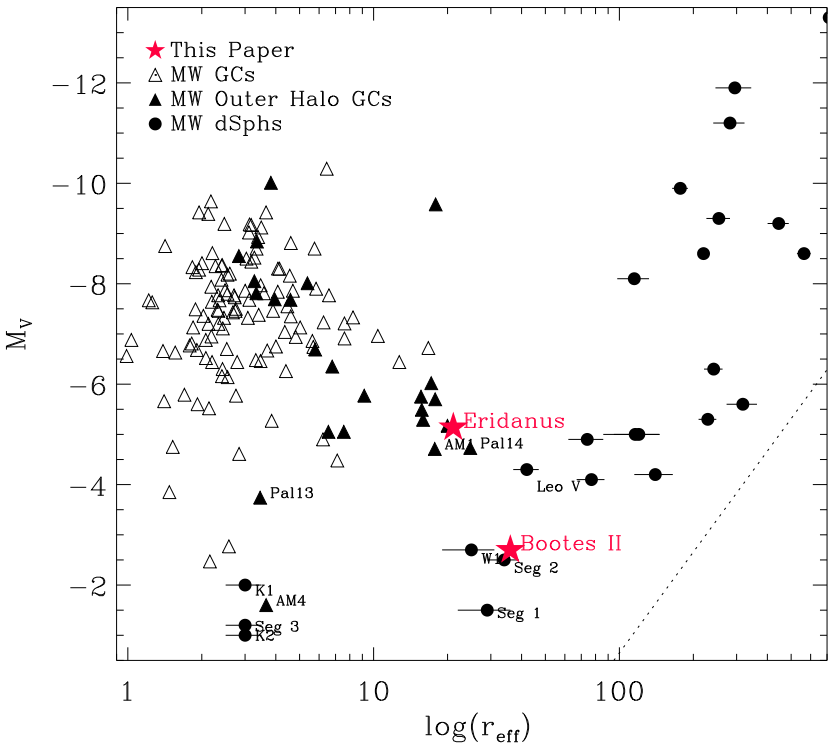

FIG. 5.— The absolute magnitude (M_V) versus half-light radius ($R_{\rm eff}$) for Milky Way dSphs (circles) and globular clusters (triangles) in the outer halo (dist $>$ 20 kpc). These systems are well separated for magnitudes brighter than $M_V < -5$, but overlap at the faintest magnitudes. The names of the globular clusters and ultra-faint dwarf galaxies near this overlap region are listed. Large red symbols indicate the position of the objects studied in this work, Boo II and Eridanus.

Faber, S. M., Phillips, A. C., Kibrick, R. I., Alcott, B., Allen, S. L., Burrous, J., Cantrall, T., Clarke, D., Coil, A. L., Cowley, D. J., Davis, M., Deich, W. T. S., Dietsch, K., Gilmore, D. K., Harper, C. A., Hilyard, D. F., Lewis, J. P., McVeigh, M., Newman, J., Osborne, J., Schiavon, R., Stover, R. J., Tucker, D., Wallace, V., Wei, M., Wirth, G., & Wright, C. A. 2003, in Society of Photo-Optical Instrumentation Engineers (SPIE) Conference Series, Vol. 4841, Instrument Design and Performance for Optical/Infrared Ground-based Telescopes, ed. M. Iye & A. F. M. Moorwood, 1657–1669

Geha, M., Willman, B., Simon, J. D., Strigari, L. E., Kirby, E. N., Law, D. R., & Strader, J. 2009, ApJ, 692, 1464

Girardi, L., Bertelli, G., Bressan, A., Chiosi, C., Groenewegen, M. A. T., Marigo, P., Salasnich, B., & Weiss, A. 2002, A&A, 391, 195

Gnedin, O. Y. & Zhao, H. 2002, MNRAS, 333, 299

Harris, W. E. 1996, AJ, 112, 1487

Kirby, E. N., Simon, J. D., Geha, M., Guhathakurta, P., & Frebel, A. 2008, ApJ, 685, L43

Koch, A., McWilliam, A., Grebel, E. K., Zucker, D. B., & Belokurov, V. 2008, ApJ, 688, L13

Martin, N. F., de Jong, J. T. A., & Rix, H.-W. 2008, ApJ, 684, 1075

Muñoz, E., Lu, J., & Yakobson, B. I. 2010, Nano Letters, 10, 1652

Muñoz, R. R., Majewski, S. R., Zaggia, S., Kunkel, W. E., Frinchaboy, P. M., Nidever, D. L., Crnojevic, D., Patterson, R. J., Crane, J. D., Johnston, K. V., Sohn, S. T., Bernstein, R., & Shectman, S. 2006, ApJ, 649, 201

Newman, A. B., Ellis, R. S., Bundy, K., & Treu, T. 2012, ApJ, 746, 162

Ortolani, S. & Gratton, R. G. 1986, A&A, 160, 25

Robin, A. C., Reylé, C., Derrière, S., & Picaud, S. 2003, A&A, 409, 523

Schlegel, D. J., Finkbeiner, D. P., & Davis, M. 1998, ApJ, 500, 525

Simon, J. D. & Geha, M. 2007, ApJ, 670, 313

Simon, J. D., Geha, M., Minor, Q. E., Martinez, G. D., Kirby, E. N., Bullock, J. S., Kaplinghat, M., Strigari, L. E., Willman, B., Choi, P. I., Tollerud, E. J., & Wolf, J. 2011, ApJ, 733, 46

Sohn, S. T., O'Connell, R. W., Kundu, A., Landsman, W. B., Burstein, D., Bohlin, R. C., Frogel, J. A., & Rose, J. A. 2006, AJ, 131, 866

Stetson, P. B. 1994, PASP, 106, 250

Stetson, P. B., Bolte, M., Harris, W. E., Hesser, J. E., van den Bergh, S., Vandenberg, D. A., Bell, R. A., Johnson, J. A., Bond, H. E., Fullton, L. K., Fahlman, G. G., & Richer, H. B. 1999, AJ, 117, 247

Walsh, S. M., Jerjen, H., & Willman, B. 2007, ApJ, 662, L83

Walsh, S. M., Willman, B., Sand, D., Harris, J., Seth, A., Zaritsky, D., & Jerjen, H. 2008, ApJ, 688, 245

Willman, B. & Strader, J. 2012, AJ, 144, 76

Wolf, J., Martinez, G. D., Bullock, J. S., Kaplinghat, M., Geha, M., Muñoz, R. R., Simon, J. D., & Avedo, F. F. 2010, MNRAS, 406, 1220

Zaritsky, D., Olszewski, E. W., Schommer, R. A., Peterson, R. C., & Aaronson, M. 1989, ApJ, 345, 759

TABLE 2
KECK/DEIMOS MULTI-SLITMASK OBSERVING PARAMETERS

Mask Name	α (J2000) (h : m : s)	δ (J2000) ($^\circ$: $'$: $''$)	Date Observed	PA (deg)	$t_{\rm exp}$ (sec)	# of slits	% useful spectra
Boo2_1	Feb 19, 2009	13:58:04.6	12:50:41.4	91	1800	41	93%
Boo2_2	Feb 19, 2009	13:58:01.2	12:50:52.1	177	7200	87	64%
Boo2_3	Feb 28, 2009	13:57:57.4	12:49:36.9	46	7200	74	54%
Boo2_4	Feb 19, 2009	13:58:29.3	12:44:38.3	44	1500	35	94%
Boo2_5	Feb 13, 2010	13:58:12.7	12:50:53.9	0	3600	124	72%
Eri_1	Feb 13, 2010	04:24:46.2	−21:12:25.0	0	3600	64	75%
Eri_2	Feb 14, 2010	04:24:50.4	−21:11:02.2	90	4800	64	61%

TABLE 3
KECK/DEIMOS VELOCITY MEASUREMENTS FOR MEMBER STARS IN BOO II AND ERI

i	Name	α (J2000) h m s	δ (J2000) $^\circ$ $'$ $''$	g mag	$(g-r)$ mag	v km s^{-1}	$v_{\rm err}$ km s^{-1}	$v_{\rm gsr}$ km s^{-1}
			Boo II Members					
1	3451635	10:06:40.5	+16:02:38.1	22.0	0.36	204.1	6.4	109.2
2	3451345	10:06:44.5	+16:01:29.4	20.7	0.27	210.5	4.0	115.5
3	3451159	10:06:44.6	+15:59:53.9	17.3	-0.01	200.4	2.2	105.5
..	..	..	..	..	..	..	..	..
			Eri Members					
1	3451597	10:06:34.8	+15:59:48.8	21.6	0.78	-161.5	2.9	-256.5
2	3451324	10:06:35.5	+16:02:21.1	17.7	0.88	1.4	2.2	-93.5
3	3451835	10:06:36.3	+16:02:46.3	23.2	1.22	-21.2	2.7	-116.1
..	..	..	..	..	..	..	..	..

NOTE. — Velocity measurements for member stars in the ultra-faint galaxy Boo II and globlar cluster Eri. We list the heliocentric radial velocity (v), velocity error ($v_{\rm err}$), and Galactocentric velocity ($v_{\rm gsr}$) for each star as determined in xx. Entries for non-members are published in their entirety in the electronic edition of the *Astrophysical Journal*.